Available online at www.sciencedirect.com
SCIENCE DIRECT®
Physica B 346–347 (2004) 27–33
PHYSICA B
www.elsevier.com/locate/physb

The $\frac{1}{8}$-magnetization plateau state in the 2D quantum antiferromagnet $SrCu_2(BO_3)_2$: spin superstructure, phase transition, and spin dynamics studied by high-field NMR

M. Takigawa[a,*], K. Kodama[a], M. Horvatić[b], C. Berthier[b,c], H. Kageyama[a,1], Y. Ueda[a], S. Miyahara[a,d,2], F. Becca[d,3], F. Mila[d]

[a] *Institute for Solid State Physics, University of Tokyo, 5-1-5 Kashiwanoha, Kashiwa, Chiba 277-8581, Japan*
[b] *Grenoble High Magnetic Field Laboratory, CNRS and MPI-FKF, 38042 Grenoble, France*
[c] *Laboratorie de Spectrométrie Physique, Université Joseph Fourier Grenoble I, St.-Martin d'Hères 38402, France*
[d] *Institut de Physique Théorique, Université de Lausanne, Lausanne CH-1015, Switzerland*

Abstract

We report the NMR observation of spin superstructure in the $\frac{1}{8}$ magnetization plateau phase of $SrCu_2(BO_3)_2$, a quasi-2D dimer singlet spin system, at high magnetic fields near 28 T. The $\frac{1}{8}$ phase is characterized by crystalization of triplets in a rhomboid unit cell with oscillating magnetization and separated from uniform phase by a first-order transition. Comparison between the Cu and B NMR spectra and theoretical calculations on the Shastry–Sutherland model enabled us to determine the three-dimensional spin superstructure. We also found that subtle structural feature of the buckling of magnetic layers produces anisotropic interactions, which lead to field-induced staggered magnetization.

PACS: 75.25.+z; 75.30.Kz; 76.60.Jx; 76.60.Cq

Keywords: $SrCu_2(BO_3)_2$; Magnetization plateau; NMR; Quantum spin systems

1. Introduction

Exploration of quantum phase transitions in spin systems induced by strong magnetic field is a remarkably fruitful area of recent research in high magnetic field, see for, e.g. Refs. [1,2]. Special attention has been paid on a class of materials which do not order magnetically down to zero temperature. These materials have a collective singlet ground state with a finite energy gap to the lowest excited state.

Heisenberg chains with integer spins, spin-ladders, and coupled spin dimers are well-known examples. Low lying excitations in these materials are $S = 1$ triplet magnons with energy dispersion $E(\mathbf{q})$ as a function of momentum $\mathbf{q}$. The minimum of the dispersion at $\mathbf{q} = \mathbf{Q}$ defines the spin-gap Δ.

*Corresponding author. Tel./fax: +81-4-7136-3225.
E-mail address: masashi@issp.u-tokyo.ac.jp (M. Takigawa).
[1] Present address: Department of Chemistry, Faculty of Science, Kyoto University, Sakyo-ku, Kyoto 606-8502, Japan.
[2] Present address: Department of Physics, College of Science and Engineering, Aoyama Gakuin University, Sagamihara, Kanagawa 299-8558, Japan.
[3] Present address: INFM-Democritos, National Simulation Centre, and SISSA, I-34014 Trieste, Italy.

0921-4526/$ - see front matter
doi:10.1016/j.physb.2004.01.014

When a magnetic field is applied, the triplets degeneracy is lifted by the Zeeman splitting. The gap to the lowest $S_z = 1$ triplet branch $\Delta - g\mu_B H$ becomes zero at the critical field $H_c = \Delta/(g\mu_B)$ and finite density of $S_z = 1$ triplets, i.e. finite magnetization, appears above H_c. The Bose–Einstein condensation should then occur at sufficiently low temperatures, where the order parameter of the macroscopic condensate $\langle a_0 \rangle$ is equivalent to the staggered magnetization $M_\perp(Q)$ perpendicular to the field. Such field-induced antiferromagnetic order has been indeed observed in a number of spin-gap systems [3,4] and is well described in the framework of Bose–Einstein condensation [5,6].

Upon further increasing the field, the magnetization does not always increase smoothly up to the saturation. Instead, in some materials, the magnetization stays constant at fractional values of the full saturation for a finite range of magnetic field [7]. At magnetization plateaus the density of triplets is kept constant against a change of the chemical potential (magnetic field), therefore, an excitation gap should appear again. Oshikawa et al. [8] developed a topological theory for magnetization plateaus in one dimension based on the Lieb-Shultz–Mattis theorem. They showed that if the total magnetization $\sum_j S_{zj}$ is a conserved quantity, an excitation gap exists only when

$$n(S - m) = \text{integer}, \quad m = \langle S_z \rangle, \tag{1}$$

where n is the periodicity of the ground state.

When the spin hamiltonian is mapped onto an interacting boson system, $S - m$ gives the number of particles per site. Therefore, this is equivalent to the commensurability condition that the particle number in a unit cell of the ground state has to be an integer. This argument was then extended to arbitrary dimensions [9]. It follows that if a magnetization plateau at a fractional value $S - m = p/q$ (p and q are mutually prime) is observed with q greater than the number of spins in a crystalline unit cell, the ground state must break the translational symmetry. Physically, such broken symmetry should result from localization of triplets forming a superlattice due to repulsive interactions. Magnetization plateaus are thus quite analogous to charge-ordered insulating states often observed in transition metal oxides [10]. In this paper, we describe the direct observation of a magnetic superlattice for the magnetization plateau state at $\frac{1}{8}$ of the full saturation in the quasi-2D spin-dimer system $SrCu_2(BO_3)_2$ by nuclear magnetic resonance (NMR) experiments at high magnetic field up to 28 T [11].

The crystal of $SrCu_2(BO_3)_2$ has a layered structure as depicted in Fig. 1(a) where the magnetic $CuBO_3$ layers and non-magnetic Sr layers alternate along the c-axis. The magnetic layers contain orthogonal dimers formed by pairs of nearest-neighbour Cu^{2+} ions each carrying spin $\frac{1}{2}$. If we consider isotropic antiferromagnetic Heisenberg exchange only between the nearest neighbour (J) and next-nearest neighbour (J') spins, we obtain the model shown in Fig. 1(b) proposed by Shastry and Sutherland two decades ago [12,13] The ground state of this model is obvious in the two limiting cases. When $J/J' \gg 1$, it reduces to a collection of dimer singlets, while if $J/J' \ll 1$, the model is equivalent to an antiferromagnet on a square lattice with a Néel order. Whether there are other phases is still an open question. It is known that for $J/J' < 0.68$ the simple product of dimer singlets is the *exact* ground state. Various experiments have established that $SrCu_2(BO_3)_2$ at zero magnetic field has the dimer-singlet ground state with the spin-gap $\Delta = 35$ K and appropriate values of the parameters are determined as $J/J' = 0.64$, $J = 85$ K.

It is also known that frustration between J and J' of the Shastry–Sutherland model strongly suppresses the kinetic energies of triplets. Indeed neutron scattering experiments have demonstrated

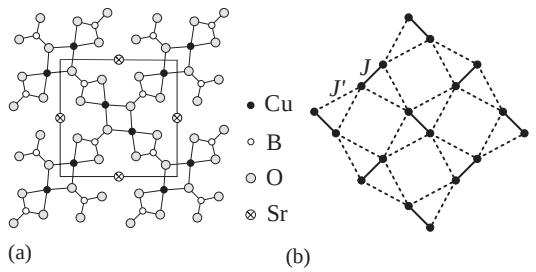

Fig. 1. (a) Schematic structure of $SrCu_2(BO_3)_2$ viewed along the c-axis. The box shows a unit cell. (b) The Shastry–Sutherland spin model.

that the dispersion of triplet magnons in $SrCu_2(BO_3)_2$ has an extremely small width [14], even though the ratio J'/J is close to the critical value. The most striking property of $SrCu_2(BO_3)_2$ is the presence of magnetization plateaus at $\frac{1}{8}$, $\frac{1}{4}$, and $\frac{1}{3}$ of the full saturation [15]. According to the commensurability condition mentioned above, the ground state at these plateaus should break the translational symmetry. The hard-core-boson calculation indeed predicted that small kinetic energies of triplets and their repulsive interactions lead to localization of the triplets to form stripe superlattices at $\frac{1}{4}$ and $\frac{1}{3}$ plateaus. For the $\frac{1}{8}$ plateau, superlattices with either square or rhomboid unit cell were proposed [18]. However, no definite conclusion was obtained concerning the stability of a specific structure [16–18].

2. Spin superstructure in the $\frac{1}{8}$ magnetization plateau phase

We have used nuclear magnetic resonance (NMR) at the Cu and B sites to detect superstructure at the $\frac{1}{8}$ plateau phase that occurs in the field range from 27 to 28.5 T when the field is applied parallel to the c-axis [11]. Since the local hyperfine field at the nuclei is determined by the interaction with neighbouring electron spins, magnetic superstructure should give rise to distinct types of nuclei with different hyperfine fields, resulting in fine structure in the NMR spectra. NMR experiments were done on a single crystal grown by the travelling solvent-floating zone method using a 20 MW resistive magnet at the Grenoble High Magnetic Field Laboratory.

First, we briefly review the Cu NMR results, which have been reported in Ref. [11]. We show in Fig. 2 the Cu NMR spectrum at the magnetic field of 26 T (below the onset of the $\frac{1}{8}$-plateau) and 27.6 T (inside the $\frac{1}{8}$-plateau) obtained near $T \sim 50$ mK. The spectrum at 26 T can be reproduced as a superposition of six lines coming from single Cu site, three lines split by quadrupole interaction for the two isotopes ^{65}Cu and ^{63}Cu, as indicated by the line in the inset. This confirms that the magnetization is largely uniform. The NMR spectrum shows a drastic change when the field is increased up to 27.6 T. There are many sharp peaks distributed over a extremely wide frequency range from 100 to over 400 MHz, pointing to many distinct Cu sites with different magnetization. This gives a direct evidence for a commensurate magnetic superstructure.

In spite of the apparent complexity of the spectrum, a large number of sharp peaks allowed us to determine the distribution of hyperfine fields quite accurately. We found that in order to reproduce all the peak positions of the spectrum, at least 11 distinct hyperfine fields have to be assumed [11]. The distribution of the hyperfine fields is shown in the middle panel of Fig. 3(b),

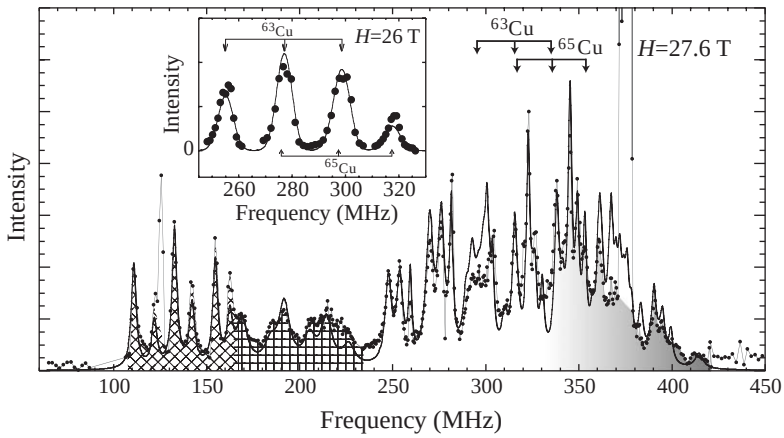

Fig. 2. The Cu NMR spectrum at 26 T (inset) and 27.6 T (main panel). The arrows in the main panel shows the reference NMR frequency in diamagnetic materials.

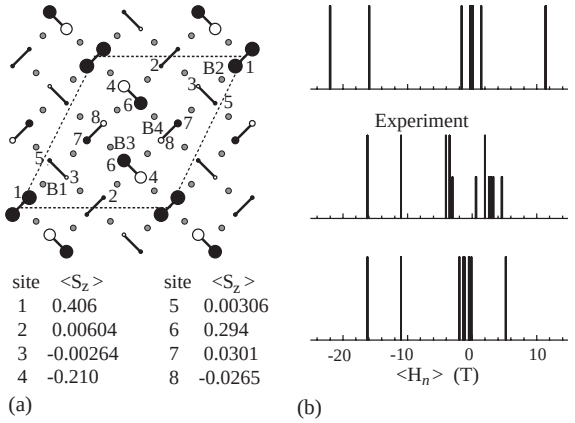

site	$\langle S_z \rangle$	site	$\langle S_z \rangle$
1	0.406	5	0.00306
2	0.00604	6	0.294
3	-0.00264	7	0.0301
4	-0.210	8	-0.0265

(a) (b)

Fig. 3. (a) Calculated magnetization profile. Hatched circles show the B sites shown for later discussion. Solid (open) circles indicate the Cu sites with magnetization parallel (antiparallel) to the external field with the circle size representing the magnitude. There are eight distinct Cu sites in one layer. The values of local magnetization are listed below. (b) Histogram of the hyperfine field distribution. The middle panel shows the experimental results, while the upper (lower) panel indicates the calculated results without (with) the transferred hyperfine coupling. See Ref. [11] for details.

where long (short) lines indicate that the population of the site is $\frac{1}{8}$ ($\frac{1}{16}$). The NMR spectrum generated from this distribution is shown by the thick line in Fig. 2. By symmetry consideration, it is concluded that only the rhomboid-type unit cell is compatible with the NMR observation of more than 11 sites [11]. The middle panel of Fig. 3(b) shows that two sites have large negative hyperfine fields, which through a negative hyperfine coupling means large magnetization along the field. Thus the triplets must be spatially extended, instead of being confined on one dimer as envisaged by the approximate treatment of hard-core-boson model [16–18]. Note also that some sites have positive hyperfine field, i.e. local magnetization opposite to the magnetic field. Therefore, the magnetization oscillates within a unit cell.

In order to gain insight into the detailed spatial magnetization profile, the Shastry–Sutherland model with spin-phonon coupling was solved for a 16-sites cluster with the periodic boundary condition appropriate for the rhomboid unit cell [11,19]. Typical result of the calculated magnetization profile is shown in Fig. 3(a). The spin-phonon coupling was included in order to select a unique ground state out of the degenerate ground state manifold [11,19]. This is physically justified since sizeable spin-phonon coupling was indeed observed by sound velocity measurements [20]. We found that the magnetization-profile depends only weakly on the spin-phonon coupling parameters and the resultant lattice displacements is less than 1%. Therefore, we speculate that the superstructure will be stable in the thermodynamic limit without the spin-phonon coupling.

The magnetization profile in Fig. 3(a) demonstrates that one "triplet" unit basically consists of three dimers; a central dimer with large parallel moments and neighbouring dimers on both sides of the central dimer with antiparallel moments. The large negative moments next to the central dimer are due to the unfrustrated exchange field from the central dimer. Similar calculations show that this unit will survive in the $\frac{1}{4}$ and $\frac{1}{3}$ plateau phases [19]. The magnetization decays rapidly as the distance from the central dimer increases. However, the oscillation persists over the entire unit cell. This is analogous to Friedel oscillations around impurities in metals or staggered magnetization near impurities in quantum spin chains [21,22] and two-dimensional superconducting cuprates [23]. The distribution of the hyperfine field obtained from the calculated magnetization-profile shows good agreement with the experimental results as shown in Fig. 3(b), in particular, when the transferred hyperfine interactions with neighbouring sites are considered.

While the Cu NMR spectrum combined with the theoretical results yielded detailed knowledge about the magnetization profile within one layer, the ^{11}B (nuclear spin $\frac{3}{2}$) NMR spectrum turned out to provide important information about the three-dimensional stacking pattern. This is because the hyperfine interactions between B nuclei and neighbouring Cu^{2+} spins are rather weak and the dipolar fields from adjacent layers are relatively important. The B NMR spectra at the field of 27.5 T are shown in Fig. 4 at three different temperatures. The spectrum at 550 mK consists of three sharp quadrupole-split lines indicating a uniform hyperfine field. On the other hand, the spectrum at 150 mK showed a large number of peaks corresponding to the superstructure in the $\frac{1}{8}$

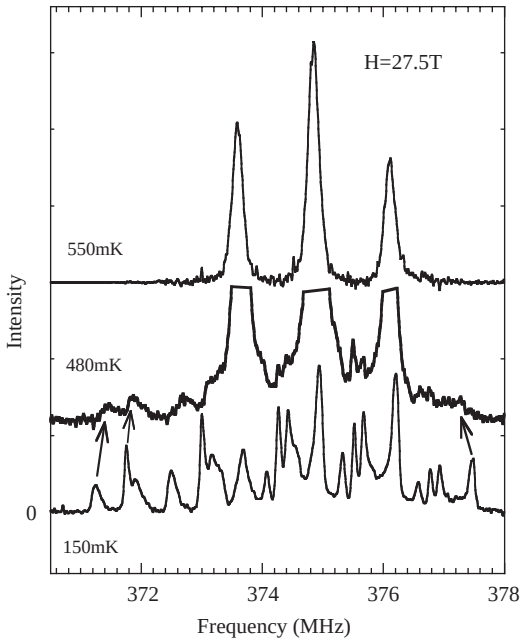

Fig. 4. The B NMR spectrum for the magnetic field of 27.5 T along the c-axis at different temperatures.

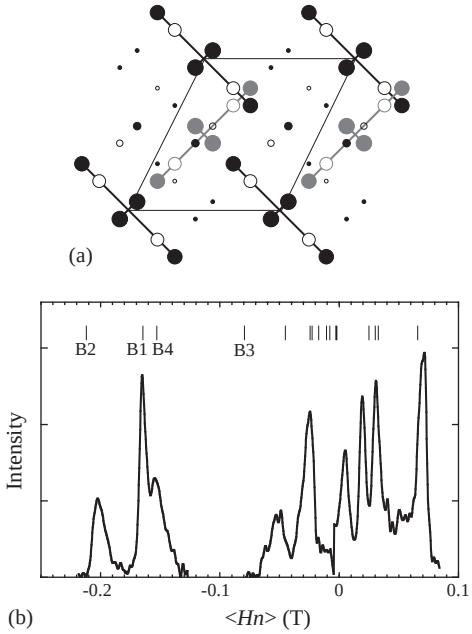

Fig. 5. (a) Three-dimensional stacking pattern of the superlattice compatible with the B NMR spectrum. The triplet units on adjacent layers are distinguished by black and grey circles. (b) Hyperfine field distribution at the B sites in the $\frac{1}{8}$ phase. Convolution of the distribution and the quadrupole structure reproduces the NMR spectrum at 150 mK. The vertical lines are the calculated results including the dipolar fields from neighbouring layers.

phase. These two types of spectra coexist at 480 mK. Close inspection of the spectrum at 150 mK allows us to generate the distribution of the hyperfine field shown in Fig. 5(b), which faithfully reproduces the observed NMR spectrum when convoluted with the quadrupole structure.

There are three peaks with large negative hyperfine fields, in contrast to the case of Cu NMR where two sites have a large negative hyperfine field. The difference should be ascribed to the dipolar fields at the B sites from neighbouring layers. We found that the B NMR spectrum can be best explained by the stacking pattern shown in Fig. 5(a). The central dimer of the triplet units in the adjacent layers are located above and below the dimer containing sites 7 and 8 shown in Fig. 3(a). Although the B1 and B2 sites in Fig. 3(a) are equivalent within one layer, the B1 site has a sizable positive dipolar field from the large moments on the neighbouring layers while the dipolar field at the B2 site is very small. Therefore, the total hyperfine field at the B1 site is much larger than the field at the B2 site. A similar situation occurs for the B3 and B4 sites. The difference in dipolar field is apparent in the calculated hyperfine field distribution shown by the lines in Fig. 5(b), which is the sum of the transferred hyperfine fields from the nearest and next nearest Cu spins and the long-ranged dipolar fields. The values of the transferred hyperfine fields are adjusted to best reproduce the experimental spectrum. This stacking pattern is consistent with the results of the hard-core boson calculation [19], which concludes that triplets on adjacent layers tend to sit as far as possible due to repulsive interaction.

3. Nature of the phase transition

We discussed the nature of the quantum phase transition into the $\frac{1}{8}$ phase in Ref. [11] based on the evolution of the B NMR spectrum as a function of magnetic field. The first-order phase transition is

demonstrated by a discontinuous jump of the magnetization deduced from the averaged hyperfine fields at the Cu sites. The order parameters of the $\frac{1}{8}$ phase is given by the spatial variation of the local magnetization, for which the overall width of the NMR spectrum provides a good measure. It was found that the spectral shape does not change in the $\frac{1}{8}$ phase at low temperatures when the field is changed, again consistent with the discontinuous transition.

The results in Fig. 4 demonstrate that the phase transition into the $\frac{1}{8}$ state as a function of temperature occurs near 500 mK for the field of 27.5 T. There is a finite range of temperature where the uniform phase and the $\frac{1}{8}$ phase coexist similar to the case of field-induced transition [11]. The width of the entire spectrum, however, decreases slightly with increasing temperature as shown by the arrows in Fig. 4. Thus the order parameter is reduced with increasing temperature, in contrast to the case of field-induced transition.

The plots in Fig. 6 show the temperature dependence of the intensity of the spectrum from the uniform phase (solid circles) and the $\frac{1}{8}$ phase (open circles). The peak height of the centre line is taken as a measure for the intensity of the uniform phase and the peak height at 372.5 MHz (at 150 mK) is plotted to present the intensity of the $\frac{1}{8}$ phase. These intensities represent the volume fraction of each phase, which varies continuously

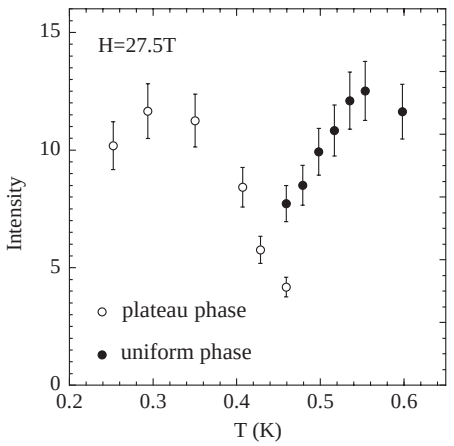

Fig. 6. Spectrae intensity of the uniform and the $\frac{1}{8}$-plateau phases plotted as a function of temperatures.

over a rather wide temperature range. The overall width of the spectrum from the $\frac{1}{8}$ phase, however, develop discontinuously, implying that the temperature induced transition is also first order.

4. The Dzyaloshinski–Moriya interaction and the field-induced staggered magnetization

Although the spin superstructure in the $\frac{1}{8}$ plateau phase is basically understood by the Shastry–Sutherland model, some properties of $SrCu_2(BO_3)_2$ cannot be explained by an isotropic Heisenberg model alone. For example, the anisotropic Dzyaloshinski–Moriya (DM) interaction on the second nearest neighbour (interdimer) bonds have to be considered in order to explain the splitting of the triplet excitation energies observed by neutron scattering [24] and electron spin resonance [25,26] experiments.

Another feature is the non-coplanar structure of the $CuBO_3$ layers. There is a structural phase transition at 395 K, below which buckling occurs in the $CuBO_3$ layers and the intradimer J bonds lose inversion symmetry [27]. This buckling results in the alternate tilting of the principal axis of the g-tensor form the c-axis toward four equivalent $\langle 1\,1\,0 \rangle$ directions on the one hand. On the other hand, it results in the intradimer DM interaction. Both of these perturbations produce an effective staggered field in the presence of a uniform magnetic field. Recently such field-induced staggered magnetization has been indeed observed by NMR experiments. We found that the orientation dependence of the B NMR frequency shift at low field (7 T) shows unusual variation with temperature. The direction at which the NMR shift is extremal moves significantly below 20 K [28]. This indicates rapid growth of the field-induced staggered magnetization at low temperatures, where the uniform magnetization becomes exponentially small.

Miyahara et al. [29] have shown that such a behaviour can be well described by considering the ground state of an isolated dimer with both the DM interaction (**D**-vector perpendicular to the magnetic field) and the alternating g-tensor. The key observation is that both interactions mix

the singlet ground state with the lowest triplet branch so that staggered magnetization linear in field appears in the lowest-order perturbation. It should be noted that the interdimer DM interaction discussed earlier [24] affects the dispersion of the triplets but does not have matrix elements between singlet and one triplet states. At sufficiently high fields, the mixing causes finite magnetization to appear below $H_c = \Delta/(g\mu_B)$ and anticrossing of the two levels at H_c, both of which appear to be relevant to experimental results. It has been indeed puzzling that the magnetization rises rather gradually below the expected H_c and there is no indication of Bose condensation of magnons, instead, the spin-gap persists above H_c [30]. It remains to be seen to what extent the simple picture derived from these anisotropic interactions captures the essential physics at high magnetic fields.

5. Summary

The spin superstructure in magnetization plateaus breaking translational symmetry was experimentally observed for the first time in the $\frac{1}{8}$ phase of $SrCu_2(BO_3)_2$. The three-dimensional spatial distribution of the magnetization was determined by combining the NMR spectrum and numerical calculations. The plateau phase is separated from the uniform phase by a first-order transition. A subtle structural feature of this compound brings anisotropic perturbations not included in the Shastry–Sutherland model, which lead to field-induced staggered magnetization.

The work is supported by Grant-in Aid for Scientific Research on Priority Area (B) on "Field-induced new quantum phenomena in magnetic systems" from Ministry of Education, Culture, Sports, Science , and Technology of Japan and the Swiss National Fund.

References

[1] C. Brthier, L.P. Levy, G. Martinez (Eds.), High Magnetic Field; Applications in Condensed Matter Physics and Spectroscopy, Springer, Berlin, 2003.
[2] T.M. Rice, Science 298 (2002) 760.
[3] H. Tanaka, et al., J. Phys. Soc. Japan 70 (2001) 939.
[4] Ch. Rüegg, et al., Nature 431 (2003) 62.
[5] T. Nikuni, M. Oshikawa, M. Oosawa, H. Tanaka, Phys. Rev. Lett. 84 (2000) 5868.
[6] M. Matsumoto, B. Normand, T.M. Rice, M. Sigris, Phys. Rev. Lett. 89 (2002) 077203.
[7] W. Shiramura, et al., J. Phys. Soc. Japan 67 (1998) 1548.
[8] M. Oshikawa, M. Yamanaka, I. Affleck, Phys. Rev. Lett. 78 (1997) 1984.
[9] M. Oshikawa, Phys. Rev. Lett. 84 (2000) 1535.
[10] T. Yamauchi, Y. Ueda, N. Mori, Phys. Rev. Lett. 89 (2002) 057002.
[11] K. Kodama, et al., Science 298 (2002) 395.
[12] B.S. Shastry, B. Sutherland, Physica B 108 (1981) 1069.
[13] [For a review on $SrCu_2(BO_3)_2$ and the Shastry-Sutherland model, see] S. Miyahara, K. Ueda, J. Phys.: Condens. Matter 15 (2003) R327.
[14] H. Kageyama, et al., Phys. Rev. Lett. 84 (2000) 5876.
[15] K. Onizuka, et al., J. Phys. Soc. Japan 69 (2000) 1016.
[16] T. Momoi, K. Totsuka, Phys. Rev. B 61 (2000) 3231.
[17] T. Momoi, K. Totsuka, Phys. Rev. B 62 (2000) 15067.
[18] S. Miyahara, K. Ueda, Phys. Rev. B 61 (2000) 3417.
[19] S. Miyahara, F. Becca, F. Mila, Phys. Rev. B 68 (2003) 024401.
[20] B. Wolf, et al., Phys. Rev. Lett. 86 (2001) 4847.
[21] M. Takigawa, N. Motoyama, H. Eisaki, S. Uchida, Phys. Rev. B 55 (1997) 14129.
[22] F. Tedoldi, R. Santachiara, M. Horvatic, Phys. Rev. Lett. 83 (1999) 412.
[23] M.-H. Julien, et al., Phys. Rev. Lett. 84 (2000) 3422.
[24] O. Cépas, et al., Phys. Rev. Lett. 87 (2001) 167205.
[25] H. Nojiri, et al., J. Phys. Soc. Japan 68 (1999) 2906.
[26] H. Nojiri, et al., cond-mat/0212479.
[27] K. Sparta, et al., Eur. Phys. J. B 19 (2001) 507.
[28] K. Kodama, et al., J. Magn. Magn. Mater., in press.
[29] S. Miyahara, et al., J. Phys.: Condens. Matter, in press.
[30] H. Tsujii, et al., cond-mat/0301509.